Chapter 5

Fabricating Micron-scale Oblique Polymer Structures by Electron Beam Writing on Resist-Coated SiO$_2$ Wafers

Abstract

We have successfully fabricated SU-8 materials having oblique structures by a new electron beam technology. We studied the contrast, sensitivity, etching, and thermal properties of SU-8, PMMA, and KrF resists to evaluate their suitability for the fabrication of oblique structures. Among these resists, SU-8 revealed the lowest contrast ratio, highest throughout, and best thermal stability, and so it became the candidate material for patterning the oblique structures. The technique we have developed involves five regional exposures of a thick SU-8 resist layer with various electron beam dosages. Furthermore, we discuss the surface morphology, reaction mechanism, and hydrophobicity after subjecting the SU-8 resist to a series of plasma treatments. The formation of surface nano-nodules during oxygen plasma treatment explains the surface hydrophobicity. We have carefully evaluated the effects of the electron beam writing dose and the design of the exposure area with respect to the inclined angle of the fabricated structure.

5.1 INTRODUCTION

Microfabricated fluidic devices are potentially useful for multidimensional separations because small sample volumes can be manipulated and highly efficient separations can be achieved. Rapid progress in the production of micromechanic, microfluidic, and microoptic devices has propelled the development of new methods for the formation of binary high-aspect-ratio structures in relatively thick resist layers by X-ray and photolithography. Most fluid channels, however, are fabricated presently using optical or soft lithographic technologies.[1–3] The development of new techniques for preparing oblique microfluidic channels will benefit future bio-device applications.[4] Sloped microfluidic structures have the advantage of having smaller chip surface areas than do planar designs having the same flow distance.

Several lithographic techniques for the production of non-planar structures have been developed, such as stereo-lithography and focused ion-beam deposition. Stereo-lithography can be used to fabricate 3-D and high-aspect-ratio microstructures with low manufacturing costs and short fabrication times. Stereo-lithography also can customize the packages for microfluidics and microsensors to eliminate the dead volume of the reaction chamber.[5] The fabrication of MEMS packages on a wafer-level scale can decrease the manufacturing and assembly times. Stereo-lithography, however, uses an optical source to illuminate the resist and so the pattern resolution is restricted. Focused-ion-beam micromachining and focused-ion-beam deposition enable spatially selective and maskless patterning and processing of materials at extremely high levels of resolution.[6–8] State-of-the-art focused-ion-beam columns that are based on high-brightness liquid-metal-ion-source (LMIS) technology are capable of forming probes that have 10-nm dimensions, with the lower limit on spot size being set by the inherent energy spread of the LMIS and

the chromatic aberration of the ion optical systems.[9] The printing speed of the ion beam-based techniques, however, is very slow and time-consuming.

Electron beam writing, in comparison with optical or soft lithography, is a promising means for controlling and patterning small features, down to sub-100-nm, and for maskless processing.[10,11] The electron beam writing technology does not require a mask or mold for a pattern to be obtained, and such technologies have potential applicability for future mass production.[12] The development of electron beam resists for channel fabrication has focused on improving the sensitivity, resolution, and etching resistance of these materials.

Poly(methyl methacrylate) (PMMA) was the first, and is still the most popular, resist for electron beam applications for fabricating MEMS.[13–15] Moreover, PMMA is a positive radiation resist that has the highest resolution of all known resists, but the lowest sensitivity to irradiation, which limits its application in submicron microelectronics technologies. This deficiency may be overcome by chemical modification of the polymer to incorporate electron-accepting substituents into its macromolecular composition. The poor resistance to corrosive etching conditions and thermal instability may, however, restrict further applications.[16] The present KrF chemically amplified resist provides fast throughput, higher etching resistance, and better printing resolution,[17] but the excellent contrast confines its applications to patterning oblique structures. An alternative, epoxy-based material, SU-8, is a solvent developed and chemically amplified resist system that has excellent sensitivity, thermal stability, and etching resistance. Conventionally, the SU-8 resist is used to fabricate planar and high-aspect-ratio patterns for micromachining systems.[18] To date, most research related to the SU-8 series of materials has concentrated on using thick or ultra-thick films, and has focused mainly on mechanical applications, using

conventional UV or X-ray exposure.[19,20] Less attention, however, has been directed toward applying electron beam irradiation to manufacturing sloped structures.

Initially, this paper describes a study that compares SU-8, PMMA, and KrF resists for their sensitivity, contrast, etching resistance, and thermal stability. Subsequently, we evaluated the surface properties and morphologies of SU-8 resists after their treatment with oxygen plasma. In addition, the electron beam writing strategy and the fabrication of oblique structures are proposed and discussed.

5.2 EXPRIMENT

The SU8-50 photoresist obtained from Microchem (MA, USA) was used to fabricate three-dimensional structures by electron beam writing. The ingredients of the resist, as provided by the vendor, are 50–70% epoxy resin, 25–50% γ-butyrolactone, 1–5% propylene carbonate, and triarylsulfonium hexafluoroantimonate salts. PMMA-A55 was also obtained from Microchem; KrF UV-86 resist was obtained from Shipley (MA, USA). Electron beam exposure was performed on a Leica Weprint Model-200 stepper (Jena, Germany). The electron beam energy was 40 kV with a beam size of 20 nm and a beam current of 40 A/cm^2. The developer for the SU8-50 photoresist was 98–100% 1-methoxy-2-propyl acetate solution. The developer for the PMMA resist was a mixture of methyl isobutyl ketone and isopropanol, while that for the KrF UV-86 resist was 2.38% tetramethylammonium hydroxide solution.

The SU8-50 resists were spin-coated onto the SiO$_2$ film of a 6-inch silicon wafer—the resist thickness was 17 μm at the spin rate of 6000 rpm for 0.5

116

min—followed a two-step soft-baking process (10 min at 65 °C, then 2 min at 90 °C). The post-exposure baking (PEB) also proceeded in two steps: 30 min at 65 °C and then 10 min at 90 °C. The film outgassing was determined using a Hitachi (Tokyo, Japan) UG-21 thermal desorption system (TDS) in conjunction with a UG-400P atmospheric-pressure-ionization mass spectrometer (APIMS). The desorption temperature program was set from room temperature to 300 °C at ramp rate of 3 °C/min. Oxygen plasma treatment was carried out in a plasma-enhanced chemical vapor deposition (PECVD) chamber (STS, UK); the operating frequency was 380 kHz and the power was 250 W. The contact angle (First Ten Angstroms Model FTA-125, VA, USA) was measured by injecting water (100 µL) on the sample surface. The spherulitic structure of the surface nano-lamellae was evaluated using an in-line Hitachi S-6280H SEM. The oblique morphology on the surface was evaluated using a Profiler P-10 (TENCOR, USA).
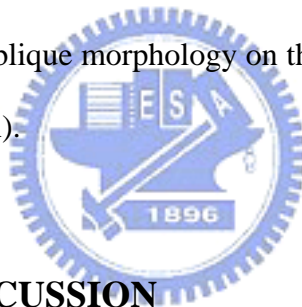
5.3 RESULTS AND DISCUSSION

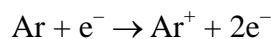### 5.3.1 Characterization of Resist Sensitivity

Characterization experiments for the three resists were carried out by electron beam exposure; the sensitivity and contrast of these resists was determined from the sensitivity curves displayed in Figure 5-1. In general, the resist having the best contrast is most suitable for patterning small features, while a resist that exhibits poor contrast is more suitable for fabricating oblique patterns. For practical mass manufacturing, the resist sensitivity can seriously affect the throughput and the cost. The samples of 17-µm-thick SU-8 film on Si-substrate were exposed with square test structures, and we measured the resist heights as a function of the applied doses. The electron beam energy was 40 keV and the doses ranged from 1 to 15 µC/cm^2 at
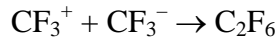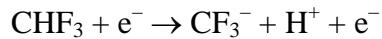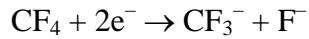
regular increments. Subsequently, these samples were baked on a hotplate and then developed. Figure 5-1 displays the sensitivity curves for three types of electronic materials. We note that the SU-8 resist changes its sensitivity and contrast when the PEB process is applied. If the PEB process of the SU-8 resist is omitted, its contrast and sensitivity decrease. As mentioned above, lower contrast is beneficial for fabricating oblique structures. The SU-8 resist has negative tone behavior upon electron beam exposure, while both PMMA and KrF UV-86 resists display positive tone behavior. We see from Figure 5-1 that the SU-8 resist has excellent sensitivity and lower contrast, regardless of its thickness. The KrF UV-86 resist has better contrast and sensitivity, while the sensitivity of the PMMA resist is too low. Therefore, of the three materials, the SU-8 resist has the best degree of flexibility in resist sensitivity and contrast and so it became our candidate for patterning oblique structures with high throughput.
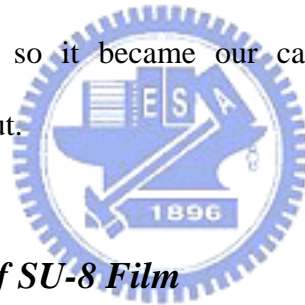
5.3.2 Etching Behavior of SU-8 Film

For fluidic channel applications, silicon dioxide materials (i.e., glass or quartz) have been suggested as substrates because of their transparency toward optical detection. In this study, we use RIE to evaluate the etching resistance for SU-8, PMMA, and KrF UV-86 resists on a silicon dioxide layer. The feeding gas is a mixture of Ar, CHF_3, and CF_4. The chemical species existing in the plasma can be expressed as follows:

$$Ar + e^- \rightarrow Ar^+ + 2e^-$$

$$CF_4 + e^- \rightarrow CF_3^+ + F^- + e^-$$

$$CF_3^+ + F^- \rightarrow CF_4$$

118

$$CF_4 + 2e^- \rightarrow CF_3^- + F^-$$

$$CHF_3 + e^- \rightarrow CF_3^- + H^+ + e^-$$

$$CF_3^+ + CF_3^- \rightarrow C_2F_6$$

$$SiO_2 + CF_3^+ + F^- \rightarrow SiF_4 + CO_2.$$

The CF_3^- and F^- species generated in the plasma react with the silicon dioxide film to form volatile species, SiF_4 and CO_2, and, through this process, the silicon dioxide film becomes etched. In addition, the generated radicals, atoms, and ions can also react with these resists to form various volatile products, such as CO, CO_2, H_2O, OH, and COF_2. Therefore, the resistance of the resist toward plasma is very important to ensure etch reliability. The etching resistance of SU-8, PMMA, and KrF UV-86 resists against CF_4 mixture gas is illustrated in Figure 5-2. Although the polymer backbones in these resists are quite different, both the SU-8 and KrF UV-86 resists exhibit better resistance, relative to the PMMA resist, during silicon dioxide etching. Increasing the CHF_3 ratio in the mixture of CHF_3 and CF_4 gases can decrease the resists etching rates as a result of the capture of reactive fluorine radicals by hydrogen radicals in the plasma. The species generated from CHF_3 in the plasma are H^+ and CF_3^-, and the CF_3^- species can quench the activity of CF_3^+ in the plasma, which results in a decreased etching rate. Otherwise, the etching selectivity (i.e., the etching rate of silicon dioxide relative to that of the resist) increases upon increasing the CHF_3 ratio, and the etching selectivity for the SU-8 film reaches almost 100 when the etching gas is CHF_3 only.

5.3.3 Thermal Stability and Reaction Mechanism

Thermal stability is another feature that favors SU-8 being used as the material,

instead of the PMMA and UV-86 resists, for oblique channel fabrication. Figure 5-3 displays the desorption behavior of various resists as determined by TDS-APIMS measurement. All of these films exhibit low out-gassing of NH_3 and C_3H_8 species. The PMMA and UV-86 films display higher H_2O desorption than does the SU-8 film during thermal stressing. The UV-86 film, when measured for C_2H_6, is thermally unstable relative to the other films, as evidenced by the extremely high out-gassing peak. In contrast, the SU-8 film exhibits very low out-gassing upon its thermal stressing. To stabilize the SU-8 film even further, we propose a technique based on an additional oxygen plasma treatment in a PECVD chamber. The inset of Figure 5-3 indicates that, after O_2 plasma treatment at 300 °C, the SU-8 film exhibits the lowest out-gassing of NH_3 and C_3H_8 species. This finding suggests that the O_2 plasma reacts with unstable species in the SU-8 film. The emitted plasma stream can penetrate the resist film and stabilize the active chemical bonds by suppressing the out-gassing effect. Taking together both its thermal stability and high etching selectivity, SU-8 seems to be a beneficial material for use in either in fluidic channel walls or in the resist process.

The triarylsulfonium hexafluoroantimonate species in the SU-8 resist is very electron-sensitive, and generates a Lewis acid upon irradiation with an electron beam. Subsequently, the low-molecular-weight epoxide ingredients (i.e., the prepolymers) undergo cationic ring-opening polymerization with the Lewis acid generated by electron irradiation or heat. This reaction propagates until a high-molecular-weight polymer forms; the product does not dissolve in the developer (1-methoxy-2-propyl acetate). This type of polymer, a thermosetting one,[21] is very resistant to plasma and thermal stressing because of its rigid network structure. Thus, the polymerization reaction in the SU-8 resist, which is initiated by a Lewis acid formed from the

triarylsulfonium hexafluoroantimonate, can be classified as a well-known chemical amplification reaction.[22] In a similar manner, KrF UV-86 is also a chemically amplified resist. Such chemically amplified resists provide high throughput because of the chain reactions they undergo. In contrast, the PMMA resist undergoes only chain scission reactions upon electron beam irradiation.[23] The direct bond scission reactions of the PMMA resist require a greater dosage for exposure.

5.3.4 Surface Properties of the SU-8 Film after Plasma Treatment

To apply the SU-8 material as a material for fabricating oblique channels, it is essential to understand its surface properties. The rule of thumb is that water-based solutions should flow through channels having hydrophilic surfaces, and nonpolar solutions in the channels that are hydrophobic. Figure 5-4 displays the contact angles for SU-8 film after various degrees of oxygen plasma treatment. The film surface exhibits hydrophobicity after being treated for 0–10 sec, but becomes hydrophilic with plasma-treatment times from 20 to 40 sec. This observation suggests that oxygen plasma oxidizes the SU-8 resists and causes hydrophilicity through the formation of hydroxyl groups on its surface. Interestingly, the surface can be restored to its initial hydrophobic property after plasma treatment for 50–60 sec. This observation suggests that oxygen plasma treatment does not just hydroxylate the surface, and that the microstructure of the film's surface needs to be investigated in-depth. This oxygen treatment technology for SU-8 materials is a very simple and easy means of altering their surface hydrophilicity. The ability to control hydrophilicity will be a powerful tool when preparing the different types of channels in the future.

Figure 5-5 illustrates SEM micrographs of the surface of the SU-8 resist after oxygen plasma treatment for 5, 20, 40, and 60 sec. The morphology observed in
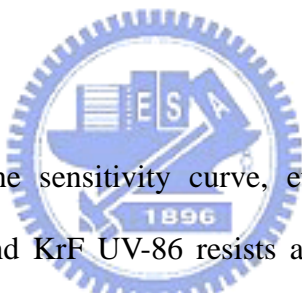
Figure 5-5a suggests that the treatment with oxygen plasma leads to the cross-linkage reaction and small cracks are formed on the surface. In Figure 5-5b (20 sec), the crack density has increased, which indicates that a large portion of the surface carbon atoms have become oxidized, and so the surface exhibits the hydrophilicity indicated in Figure 5-4. In Figure 5-5c, however, we observe nano-nodular structures have appeared after 40 sec of plasma treatment. These nano-nodules have diameters of ca. 22 nm, and the surface is hydrophilic. When the film was plasma treated for 60 sec, its surface reverted back to its hydrophobic character. The diameters of nodules increased to ca. 27 nm. It is obvious that the density of the nano-nodules plays an important role in determining the surface hydrophilicity. The nano-nodules on the surface seem to possess hydrophobic character, while the other surface, possessing with hydroxyl groups after oxygen plasma treatment, exhibits hydrophilicity. In Figure 5-5c, the role of the hydrophilic surface dominates over that of the nano-nodules, and the contact angle measurement indicates the surface's overall hydrophilicity. In contrast, the nano-nodules in Figure 5-5d cover a large portion of the surface, which, consequently, possesses hydrophobic character.

5.3.5 Fabrication of Oblique Structures

We propose a technique, illustrated in Figure 5-6, for fabricating oblique structures. The method uses an electron beam to expose a desire area, which is divided into five dosage strips, named I, II, III, IV, and V. After much experimentation with the variables, we found that dosages of 2, 2.8, 3.6, 4.8, and 12 μC/cm^2 for these strips, respectively, cause an actual sloped structure to be created on the SU-8 material. The angle of inclination of the structure depends strongly on the unit distance; this angle decreases with increasing unit distance as a result of the dose absorption per

unit area. Table 5-1 lists the mathematical fitting of the various oblique lines in Figure

5-6. The slope of the fitting equation can reflect the angle of inclination. The SEM

micrographs presented in Figure 5-7 provide further evidence that verifies the success

of this unique technique. Clearly, oblique structures having a variety of inclined

angles can be fabricated by electron beam exposure of the SU-8 material. These

oblique structures are not easy to fabricate by conventional optical illumination

methods. After their fabrication, these oblique patterns can be used as transfer molds

for imprint technology or soft lithography. Together with the oxygen plasma treatment

technology mentioned earlier, the fabrication of oblique structures is a very promising

technology for patterning hydrophilic and hydrophobic surfaces.

5.4 CONCLUSIONS

We have investigated the sensitivity curve, etching resistance, and thermal

duration of SU-8, PMMA, and KrF UV-86 resists after electron beam lithography.

The SU-8 resist demonstrates good performance in patterning oblique structures as a

result of its lower contrast, higher throughput, better etching resistance, and excellent

thermal properties, relative to the PMMA and KrF UV-86 resists. The surface of the

SU-8 film displays interesting responses to oxygen plasma treatment. The initial

surface, which is hydrophobic, becomes hydrophilic after plasma treatment for 20–40

sec, but its to hydrophobic character is restored after 50–60 sec of plasma treatment.

The formation of surface nodules, as evidenced by SEM, can be used to reasonably

explain the transformations in surface hydrophobicity. We have demonstrated a novel

gradient writing strategy that uses electron beam exposure to fabricate a sloped

structure. The inclined angle of the structure was found to have an inverse relationship

with respect to the dose received per unit area. Cross-sectional SEM images clearly

indicate that the writing strategy we have proposed can be used successfully to fabricate obliquely patterned structures.

REFERENCES

1. P. Wilding; L. J. Kricka; J. Cheng; G. Hvichia; M. A. Shoffner; P. Fortina. *Anal. Biochem.*, **257**, 95 (1998).

2. T. Deng; F. Arias; R. F. Ismagilov; P. J. A. Kenis; G. M. Whitesides. *Anal. Chem.*, **72**, 645 (2000).

3. A. J. Gawron; R. S. Martin; S. M. Lunte; *Eur. J. Pharm. Sci.*, **14**, 1 (2001).

4. N. Gottschlich; S. C. Jacobson; C. T. Culbertson; J. M. Ramsey; *Anal. Chem.*, **73**, 2669 (2001).

5. Y. M. Huang; C. P. Jiang. *Int. J. Adv. Manuf. Tech.*, **21**, 649 (2003).

6. K. J. Boyd; A. Lapicki; M. Aizawa; S. L. Anderson; *Rev. Sci. Instrum.*, **69**, 4106 (1998).

7. R. G. Woodham; H. Ahmed. *J. Vac. Sci. Technol.B*, **17**, 3075 (1999).

8. S. Reyntjens; R. Puers. *J. Micromech. Microeng.*, **10**, 181 (2000).

9. S. T. Davies; B. Khamsehpour. *Vacuum*, **47**, 455 (1996).

10. L. A. Tse; P. J. Hesketh; D. W. Rosen. *Microsyst. Technol.,* **9**, 319 (2003).

11. H. L. Chen; C. H. Chen; F. H. Ko; T. C. Chu; C. T. Pan; H. C. Lin. *J. Vac. Sci. Technol.B,* **20**, 2973 (2002).

12. Semiconductor Industry Association, *International Technology Roadmap for Semiconductor*, 2002 Updated, SIA Publication (2003).

13. F. De Carlo; D. C. Mancini; B. Lai; J. J. Song. *Microsyst. Technol.*, **4**, 86 (1998).

14. Y. Chen; D. Macintyre; S. Thoms. *J. Vac. Sci. Technol. B*, **17**, 2507 (1999).

15. A. C. F. Hoole; M. E. Welland; A. N. Broers. *Semicond. Sci. Technol.* **12**, 1166 (1997)

16. M. J. Rooks; E. Kratschmer; R. Viswanathan; J. Katine; R. E. Fontana; S. A.

MacDonald. *J. Vac. Sci. Technol.B*, **20**, 2937 (2002).

17. H. Ito. *IBM J. Res. & Dev.*, **45**, 683 (2001).

18. H. Lorenz; M. Despont; N. Fahrni; N. LaBianca; P. Renaud; P. Vettiger. *J. Micromech. Microeng.*, **7**, 121 (1997).

19. H. Lorenz; M. Despont; P. Vettiger; P. Renaud. *Microsyst. Technol.*, **4**, 143 (1998).

20. J. R. Hall; C. A. L. Westerdahl; A. T. Devine; M. J. Bodnar. *J. Appl. Polym. Sci.*, **13**, 2085 (1969).

21. R. J. Young; P. A. Lovell. *Introduction to Polymers*, 2nd Ed., Chap 1, Chapman & Hall, London (1991).

22. J. K. Chen; F. H. Ko; H. K. Chen, C. T. Chou, H. L. Chen; F. C. Chang. *J. Vac. Sci. Technol. B*. **22(2)**, 492 (2004).

23. J. O. Choi; J. A. Moore; J. C. Corelli; J. P. Silverman; H. Bakhru. *J. Vac. Sci. Technol.*, *B. 6*, 2286 (1988).
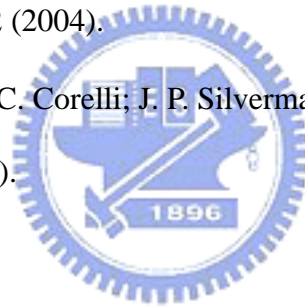
Table 5-1. The fitting equation for various electron beam writing strategies.

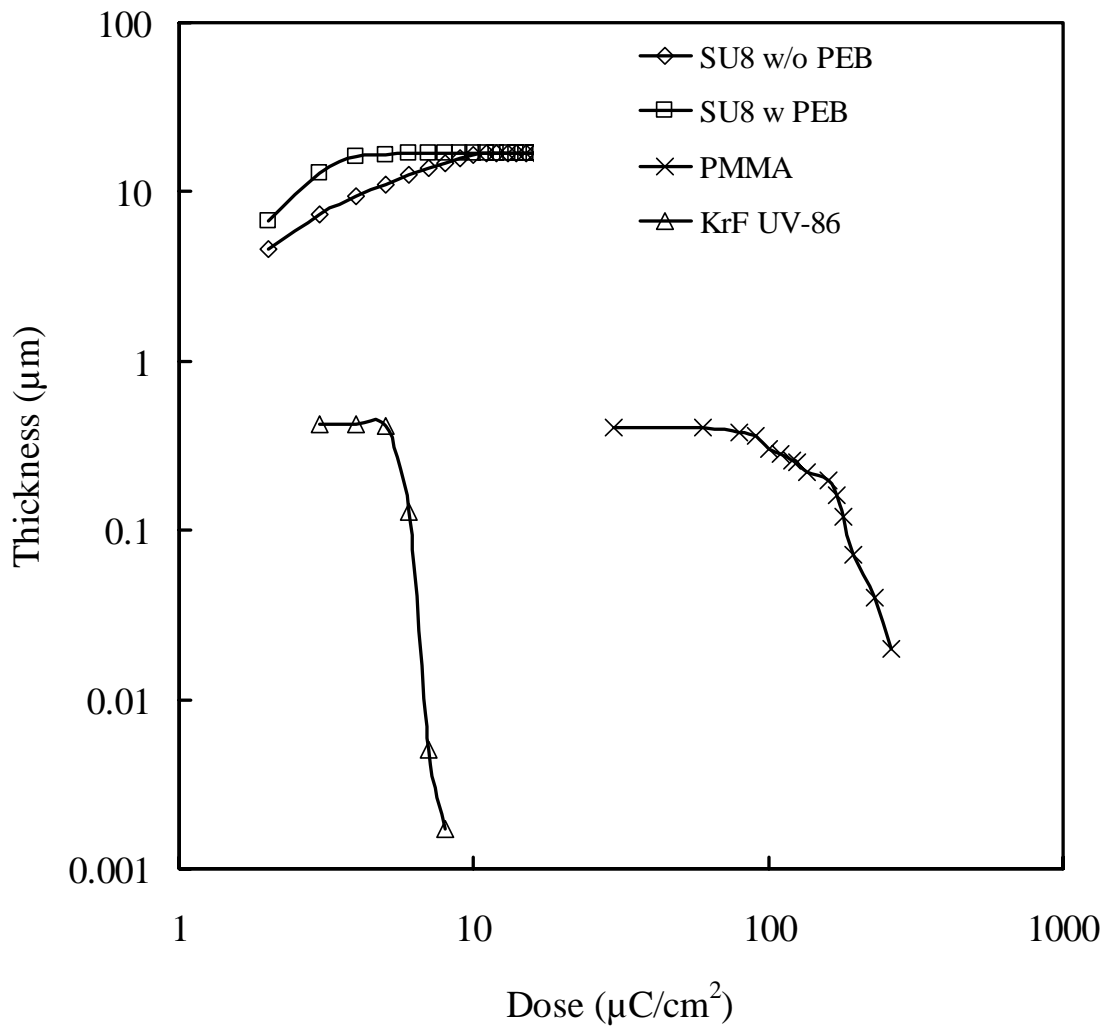| Unit distance	Fitting equation [Y: thickness (μm); X: scanning distance (μm)]
3 μm	Y = 1.118X
5 μm	Y = 0.77X
7 μm	Y = 0.448X
9 μm	Y = 0.33X
15 μm	Y = 0.188X
20 μm	Y = 0.139X
25 μm	Y = 0.107X

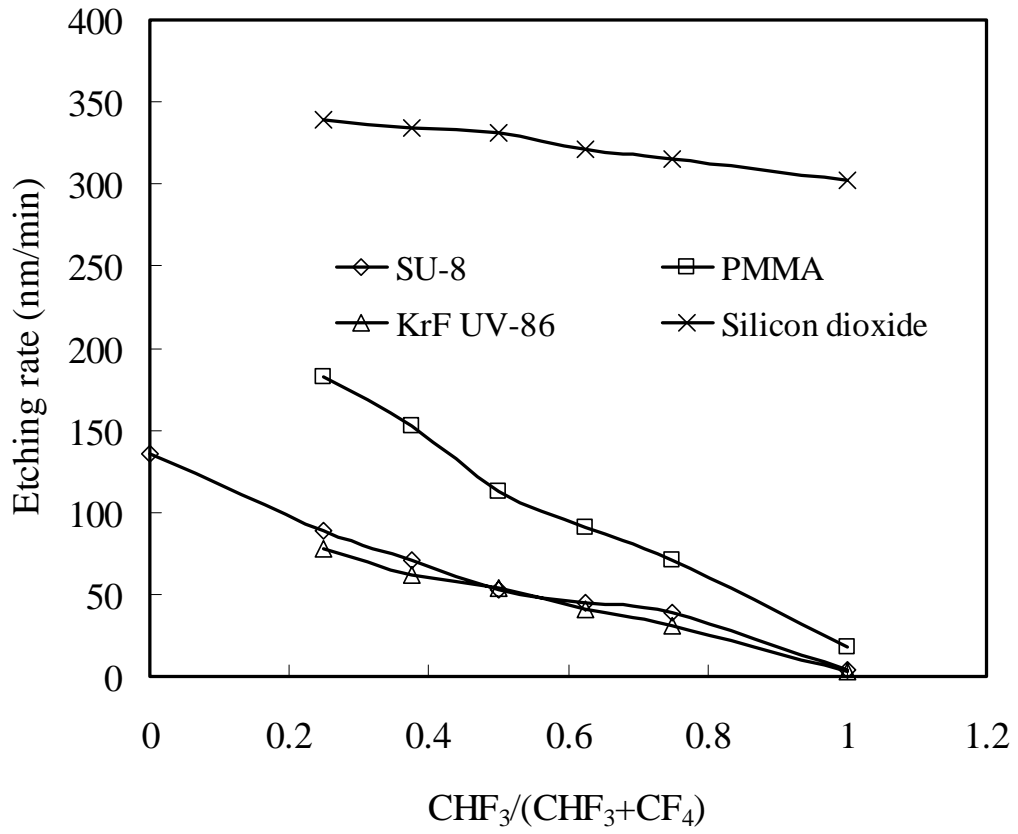**Figure 5-1**. The effect of the electron beam dose on the thickness of the resist.

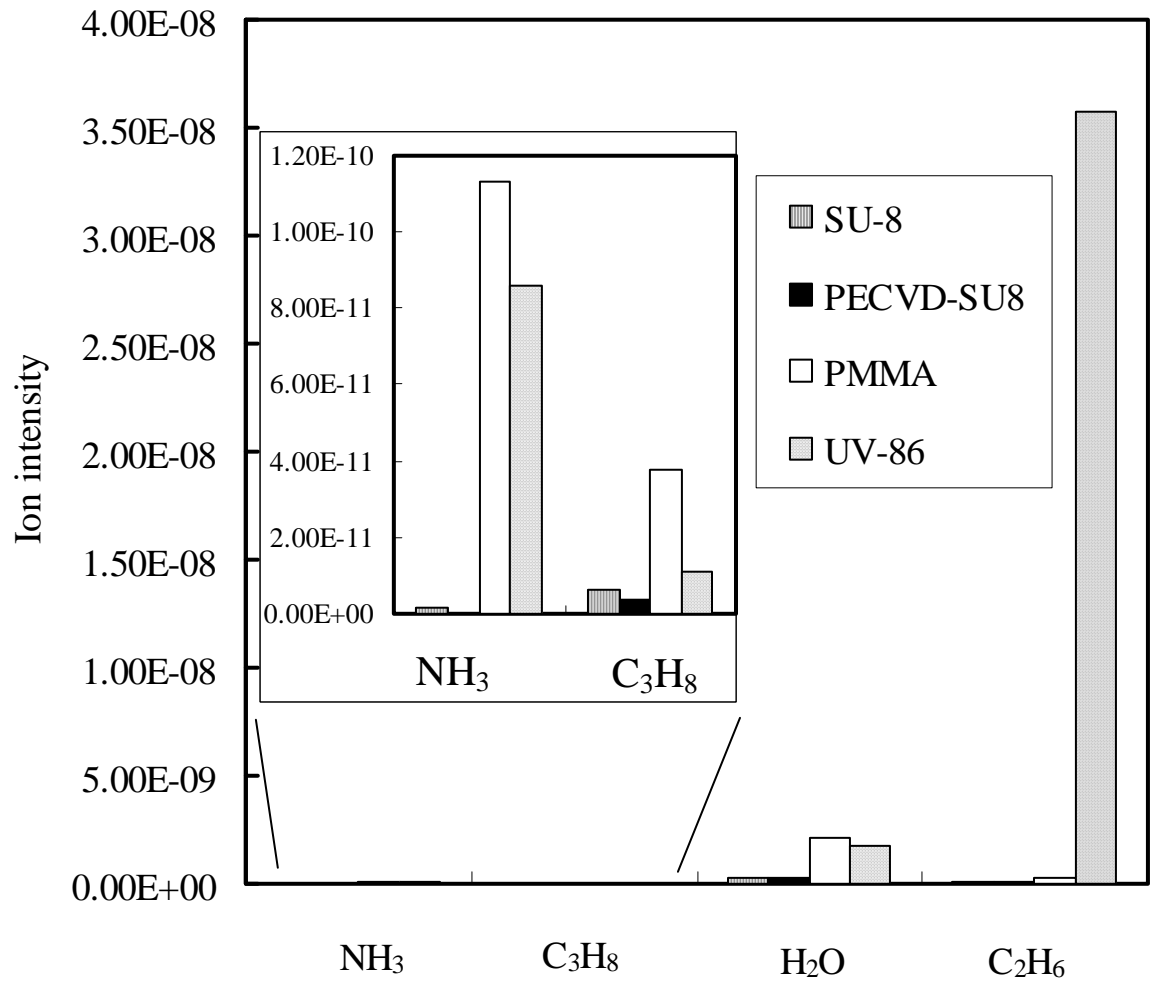**Figure 5-2**. The effect of the etching gas composition on the etching rate.

Figure 5-3. The thermal stability of various resists (oxygen plasma treatment for SU-8 resist in a PECVD chamber at 300 °C).
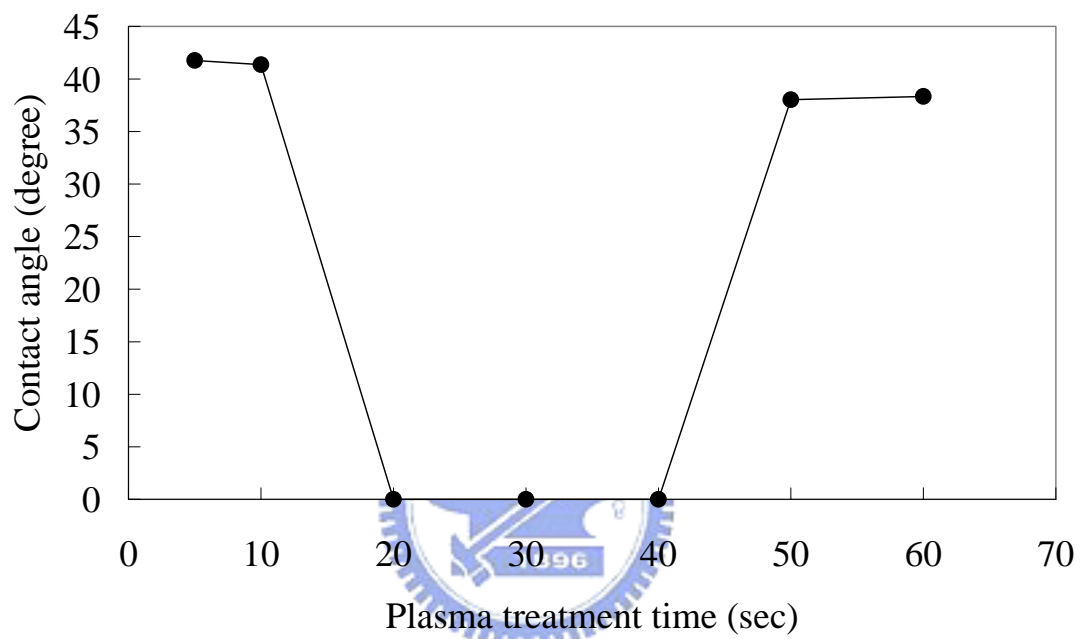
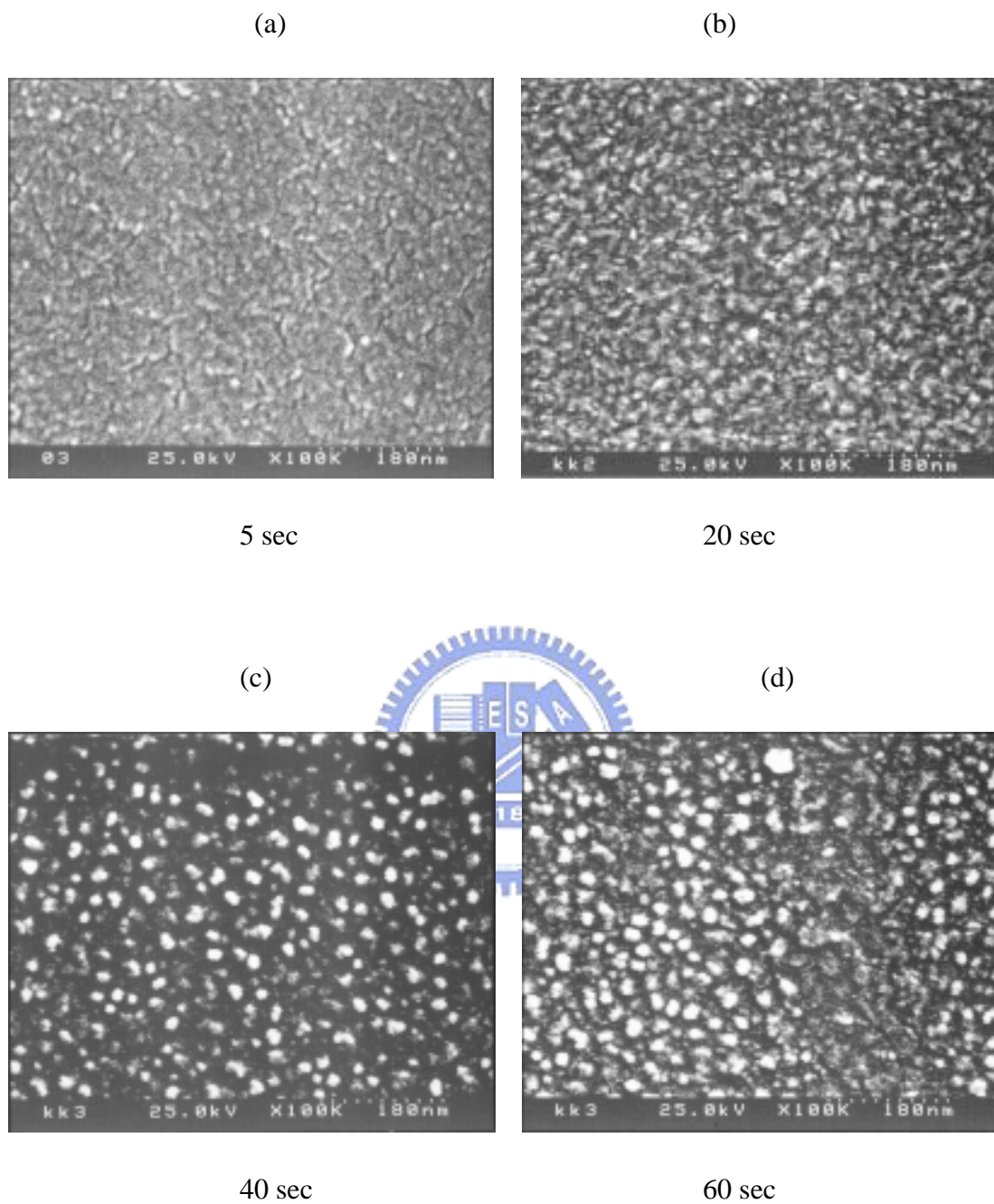**Figure 5-4**. The effect of oxygen plasma-treatment time on the contact angle of the

SU8-50 film.

(a)

(b)

5 sec

20 sec

(c)

(d)

40 sec

60 sec

Figure 5-5. SEM images (plan views; 10^5 magnification) of oxygen plasma-treated

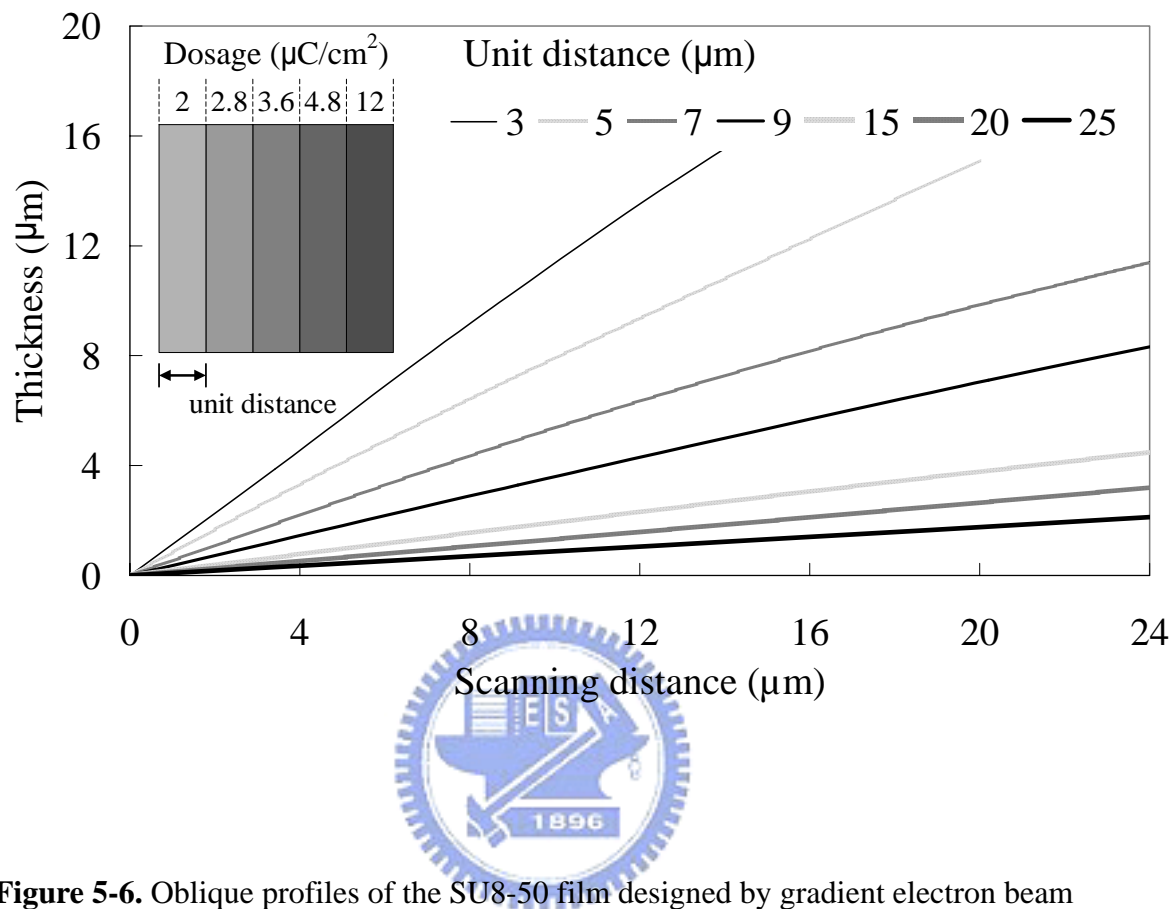SU8-50 resist films after treatment for (a) 5 s, (b) 20 s, (c) 40 s, and (d) 60 s.

Figure 5-6. Oblique profiles of the SU8-50 film designed by gradient electron beam exposure.

(a)   (b)

(c)   (d)
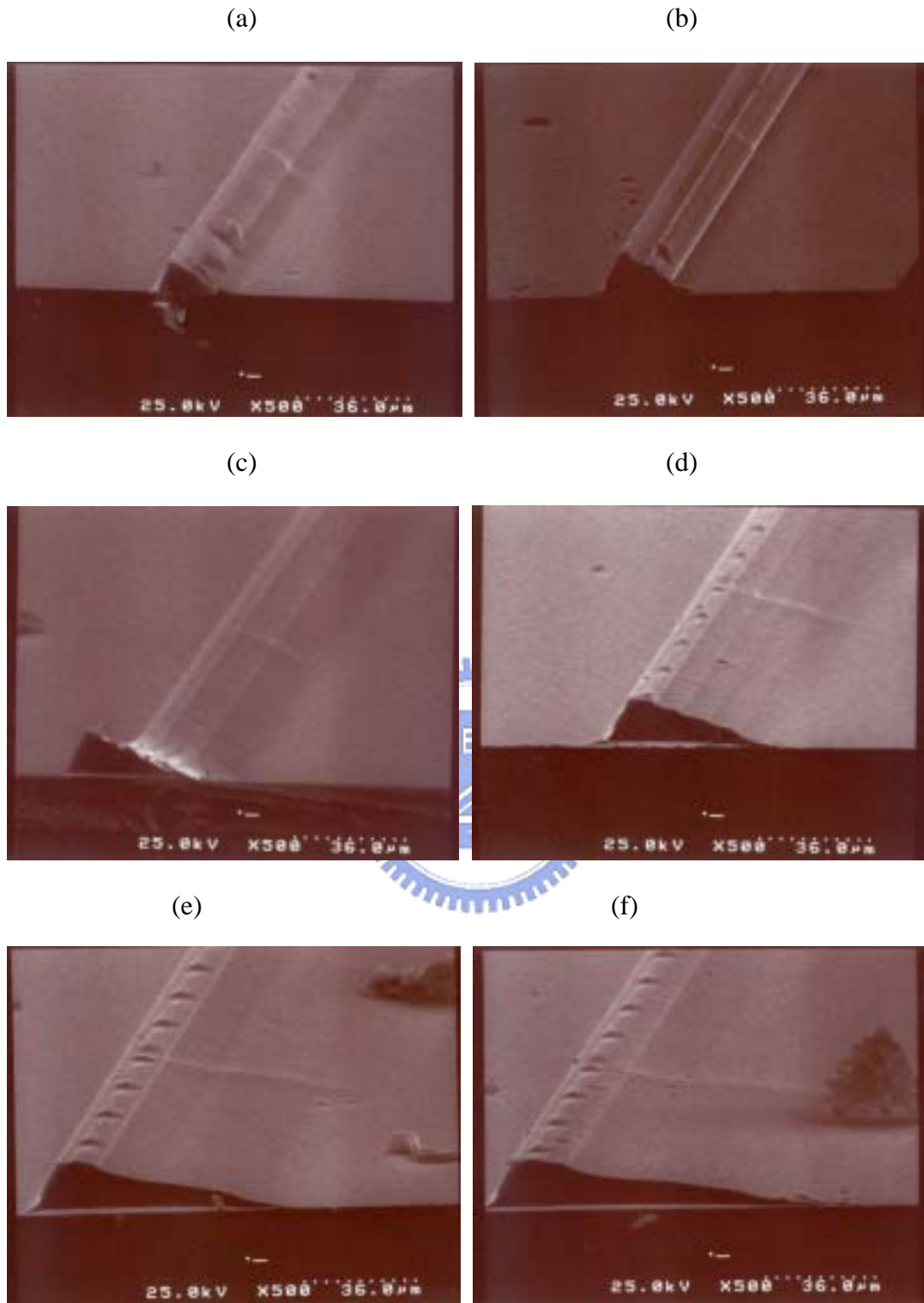
(e)   (f)

Figure 5-7. SEM images of the oblique profiles of the SU8-50 film that were designed with sectional distances of (a) 3 μm, (b) 5 μm, (c) 7 μm, (d) 9 μm, (e) 15 μm, and (f) 20 μm.